Supporting Information

High-Resolution Analysis of Small Silver Clusters by Analytical Ultracentrifugation

Cornelia M. Schneider, Helmut Cölfen*

Physical Chemistry, University of Konstanz, Universitätsstraße 10, D-78457 Konstanz, Germany,

E-mail: Helmut.Coelfen@uni-konstanz.de

Table of Contents

1. Experimental

Synthesis of Ag Clusters

The silver clusters were prepared based on a recipe from Henglein et al. [1] with slight variation. $AgClO_4$ (2.1 mg, 0.01 mmol) was dissolved in 10 mL H_2O to give a 1 mM solution. Sodium polyacrylate, NaPAA (10.2 mg, 2 µmol), was weighed into a Schlenk flask and dissolved in 1.8 mL H_2O under vigorous stirring. Then 0.2 mL of the 1 mM $AgClO_4$ solution were added under stirring, to give a total of 2 mL of a 0.1 mM $AgClO_4$ and 1 mM NaPAA. The solution was deaerated by a threefold freeze-pump-thaw cycle and kept under nitrogen. $NaBH_4$ (3.8 mg, 0.1 mmol) was dissolved in 10 mL H_2O, giving a 10 mM solution, inherently oxygen-free. 10 µL of this freshly prepared solution was added under nitrogen after 2 hours to the $AgClO_4$/NaPAA solution. Within 1 s, slight yellow coloring of the solution indicated the formation of the silver clusters. Silver clusters used for AUC measurements were prepared according to this recipe. For the UV/vis study, concentrations were varied slightly from this recipe, which is mentioned directly in the results section.

Materials

$AgClO_4$ and sodium polyacrylate, M_w = 5100 g/mol, were purchased from Aldrich, $NaBH_4$ was purchased from Roth. All chemicals were used as received. For all solutions and measurements water of Milli-Q quality was used, sourced from a Milli-Q Synthesis A10 system equipped with a Quantum EX Ultrapure Organex cartridge (Millipore).

Instruments and experiments

For the AUC experiments with the silver clusters, an UV/vis multiwavelength (MWL) AUC was used. The general setup has been described in literature.[2-5] The measurement was performed at 25°C and 60 000 rpm. For a standard AUC sedimentation velocity experiment, measurement cells equipped with a 12 mm standard titanium centerpiece (Nanolytics, Potsdam, D) were used. To free the cell atmosphere from oxygen as far as possible, the assembled cell was flushed with nitrogen through the filling holes and directly filled and closed afterwards. The reference sector was filled with 350 µL of H_2O, the sample sector with 330 µL of the prepared Ag Cluster solution without purification. For the experiment on pure NaPAA, the experiment was conducted on a standard Beckman Optima XL-I, using the interference optics. The measurement was performed at 25°C and 60 000 rpm. For a standard AUC sedimentation velocity experiment, measurement cells equipped with a 12 mm standard titanium centerpiece and interference window slits were used. 330 µL of a 2 mM NaPAA solution in water was filled into the sample sector, 350 µL H_2O into the reference sector. For the experiment of NaPAA in D_2O, 330 µL of a 2 mM NaPAA solution in D_2O was filled into the sample sector, 350 µL H_2O into the reference sector. To check for concentration dependency, another experiment was conducted using 330 µL of a 1 mM NaPAA solution in D_2O in the sample sector and 350 µL H_2O in the reference sector.

For UV/vis spectroscopy a Varian Cary 50 UV/vis spectrometer was used, controlled by the software Varian UV Scan Version 3.99 (339). Samples of a volume of 600µL were drawn from the reaction vial and measured in a quartz cuvette.

For the pH measurement, a pH electrode from Mettler Toledo was applied and 2 mL of each solution was used for the measurement (pure 1 µM NaPAA solution in water, silver clusters in water as received from synthesis).

For high-resolution transmission electron microscopy (HR-TEM), a JEOL JEM-2200FS microscope with an acceleration voltage of 200 kV was used. 1 µL of the silver cluster solution was dropped onto a carbon coated copper grid without purification. Therefore, drying effects cannot be excluded.

Data analysis

The received AUC raw data of the silver clusters were analyzed using ULTRASCAN[6] and SEDFIT[7]. For the density of the solvent, 0.99704 g/mL was used, for the viscosity of the solvent 0.00891 P was used (values for H_2O at 25°C) and for $\bar{v}$, the reciprocal density, of the analyte 0.59 mL/g was used.

In ULTRASCAN, the method PCSA[8] was applied with the constraint decreasing sigmoid (PCSA-DS). This constraint is a reasonable correlation between sedimentation coefficient and $\bar{v}$ and gave a good fit quality. The grid limits were set up as follows: sedimentation coefficient: 0.2 – 5 S, $\bar{v}$: 0.4 – 0.9. Fixed value was f/f_o=1.5 or 1.6, which resulted in the best RMSD values. Analysis was performed for every third wavelength between 250 nm and 600 nm. For the Monte-Carlo analysis, 50 Monte-Carlo iterations were performed. Spectra according to the species could be extracted by the tool "view multiwave-length s spectra", which is implemented in the program.

In SEDFIT[7], a 2D analysis using the "continuous c(s,f/f_o)" tool was used to fit for both the sedimentation coefficient and the frictional ratio. This is based on a Matlab supplement to Sedfit already presented in literature[9], which was slightly modified by Ong Khac Quy, EPFL Lausanne. It allows to determine the 2D distribution in sedimentation coefficient and frictional ratio, and additionally allows to calculate the density out of these values. The limits for the analysis were set as follows: sedimentation coefficient: 0.2 – 5 S, frictional ratio: 1-3. The input value for $\bar{v}$ was 0.58 mL/g.

For the analysis of the AUC data received from both NaPAA experiments, the tool "non-interacting discrete species" from SEDFIT and ULTRASCAN PCSA with the constraint "Horizontal line", which corresponds to the c(s) analysis of SEDFIT, was used. Fit limits were set as follows: sedimentation coefficient: 0.01-5 S, $\bar{v}$: 0.3 – 0.98, fixed value was f/f_o = 1.25. For the experiment performed in water, values for density and viscosity as presented above were used. The experiment in D_2O applied the following values: For the density of the solvent, 1.10457 g/mL was used, for the viscosity of the solvent 0.01095 P was used (values for D_2O at 25°C)

For the calculation of the core size of the silver clusters, a core-shell model was applied[10], which is explained in more detail in the main text and in the Supporting Information 5.

2. UV/vis spectra of the silver clusters

Different reaction conditions for the synthesis of the silver clusters were studied by UV/vis spectroscopy:

a) Variation of the $AgClO_4$ concentration

The other parameters were: [NaPAA]= 1 mM, [$NaBH_4$] = 1 eq, 20 µL 10 mM solution

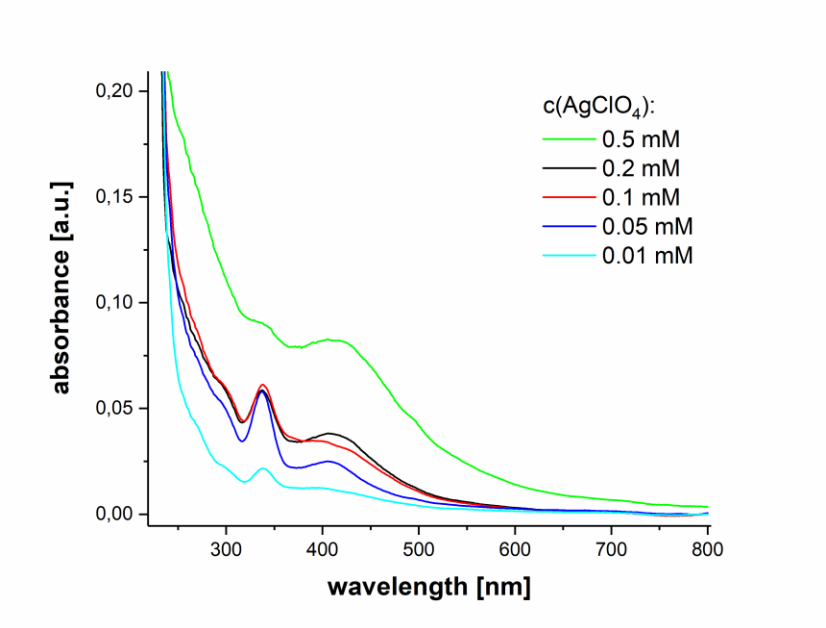

Figure S1: UV/vis spectra of the silver clusters, whereby different concentrations of AgClO4 were used. The impact on the clusters is shown by the peak characteristics.

b) Variation of the amount of sodium borohydride

The other parameters were: [NaPAA]= 1 mM, [$AgClO_4$] = 0.2 mM, the concentration of the $NaBH_4$ solution was 10 mM, 1 eq. refers to 20 µL, 0.5 eq refers to 10 µL and 1.5 eq to 30 µL volume.

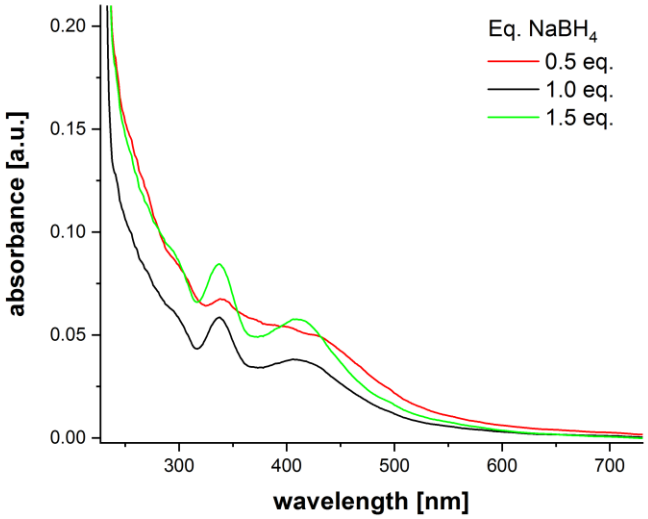

Figure S2: UV/vis spectra of the silver clusters. Different equivalents of the reduction agent sodium borohydride and the impact on the spectra characteristics were studied.

c) Variation of the concentration of NaPAA

The other parameters were: [$AgClO_4$] = 0.2 mM, [$NaBH_4$] = 1 eq, 20 µL 10 mM solution

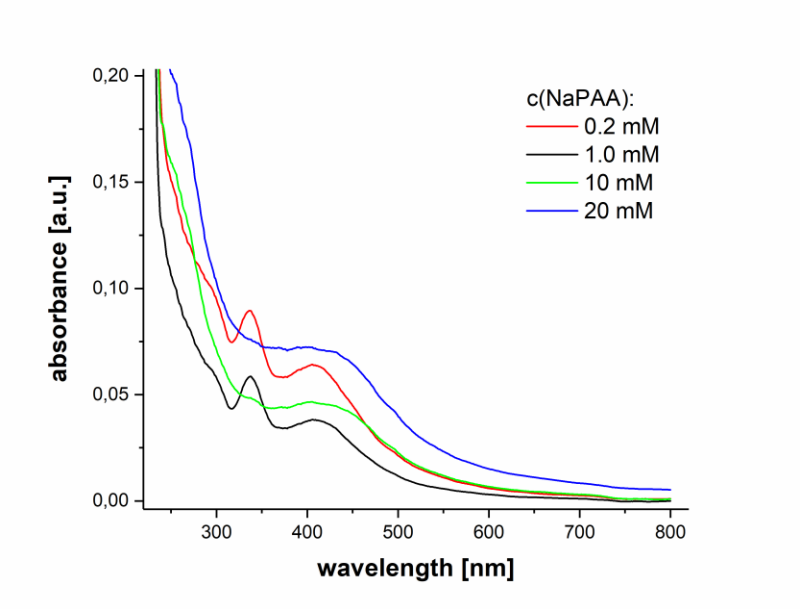

Figure S3: UV/vis spectra of the silver clusters synthesized with different concentrations of the surfactant NaPAA.

The formation of the silver clusters was also followed by titration of sodium borohydride into the solution of $AgClO_4$ and NaPAA with in situ UV/vis microscopy:

The other parameters were: [$AgClO_4$] = 0.2 mM, [NaPAA] = 1 mM

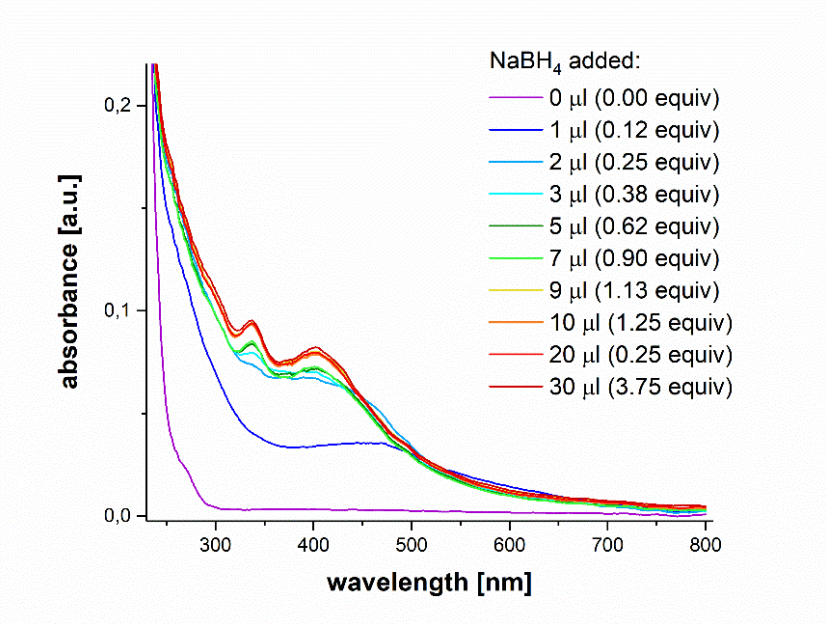

Figure S4: UV/vis spectra recorded during the titration of sodium borohydride into AgClO4 and NaPAA to directly observe the formation of silver clusters and the UV/vis band development.

3. Characterization of sodium polyacrylate

An Analytical Ultracentrifugation (AUC) experiment on NaPAA was performed and the raw data are shown in Figure S5.

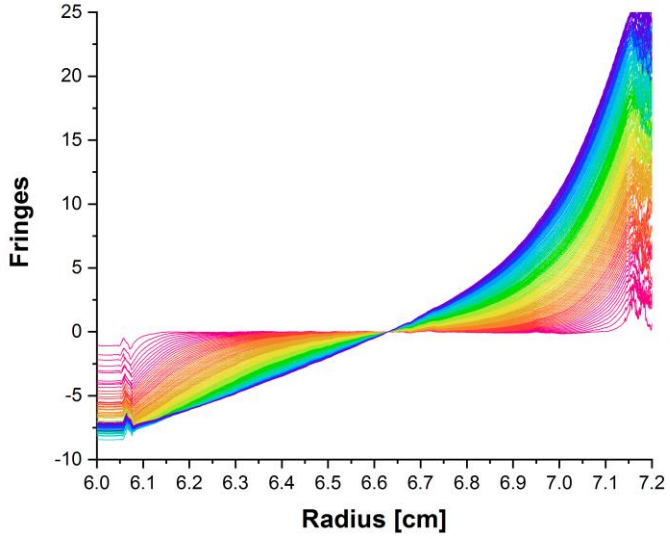

Figure S5: AUC raw data of an experiment of the pure surfactant NaPAA. Shown are the interference raw data.

Analysis of the AUC data of NaPAA in water using SEDFIT "non-interacting discrete species" on three datasets gives the fits and residuals graphed in Figure S6.

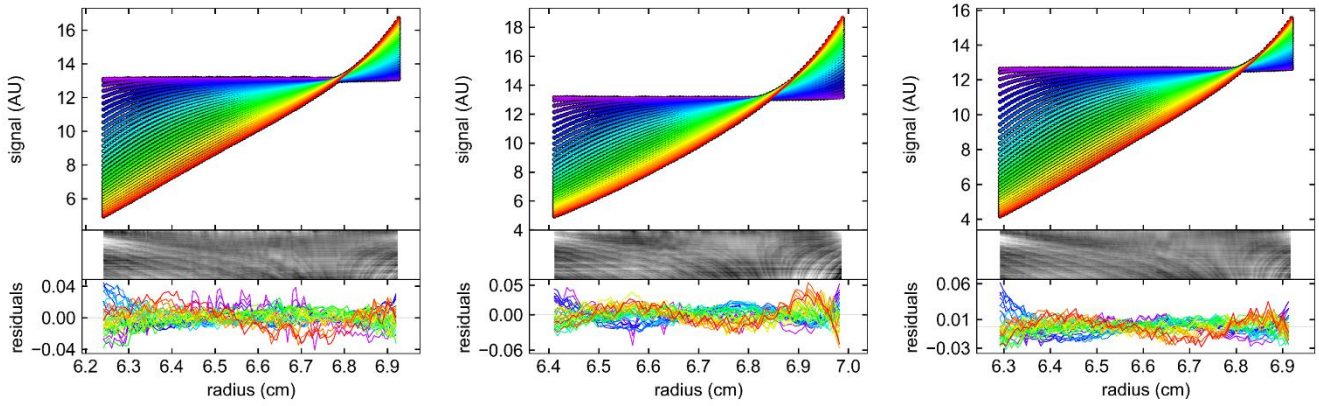

Figure S6: Data fits and residual plots of the analysis of the AUC data of 2 mM NaPAA in H_2O using SEDFIT "non-interacting discrete species".

Analysis of the AUC data of NaPAA in D_2O using SEDFIT "non-interacting discrete species" on three datasets gives the fits and residuals graphed in Figure S7.

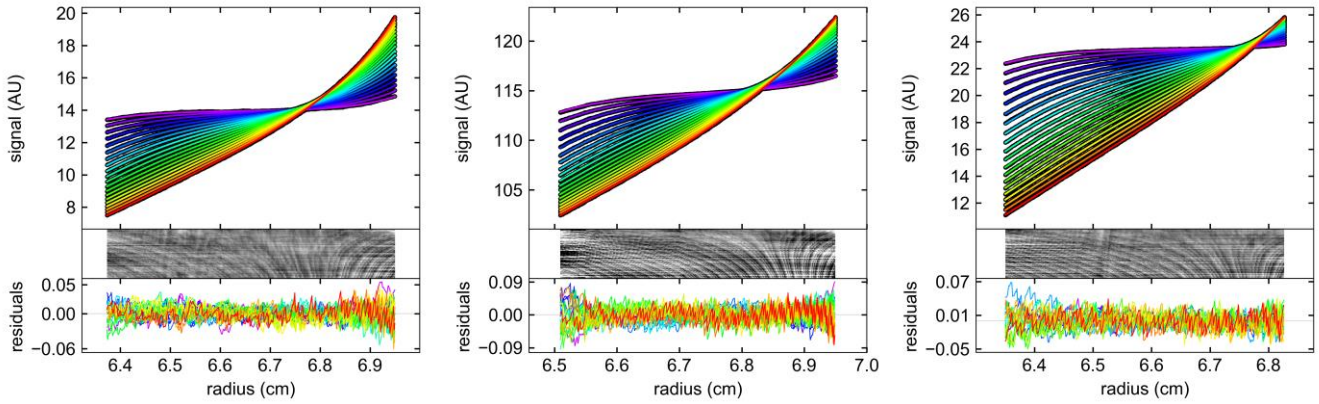

Figure S7: Data fits and residual plots of the analysis of the AUC data of 1 mM (left) and 2 mM NaPAA (middle and right) in D_2O using SEDFIT "non-interacting discrete species". The found discrete species were 0.49 S for 1 mM solution, and 0.49 S as average for the 2 mM solution.

Analysis of the data was also conducted using ULTRASCAN PCSA-HL. In order to fit for the density, the shape factor, expressed by the frictional ratio f/f_0, was held constant at 1.25, which corresponds to a shape slightly deviating from a sphere. The corresponding pseudo 3D plots of the fits of the data, which show the resulting species and $\bar{\nu}$, are shown in Figure S8. The analysis of the three data sets shows rather good agreement. As mean values for the main species for NaPAA the following values were found: sedimentation coefficient $s_{20,w}$: 0.60 ± 0.05 S, $\bar{\nu}$ = 0.872 ± 0.01 mL/g, which corresponds to a density of 1.15 g/mL. This is also in good agreement with the values from SEDFIT ($s_{20,w}$ = 0.63 S), because ULTRASCAN directly transforms the actual s value (which is normally received from SEDFIT) to $s_{20,w}$, which is corrected for temperature and solvent.

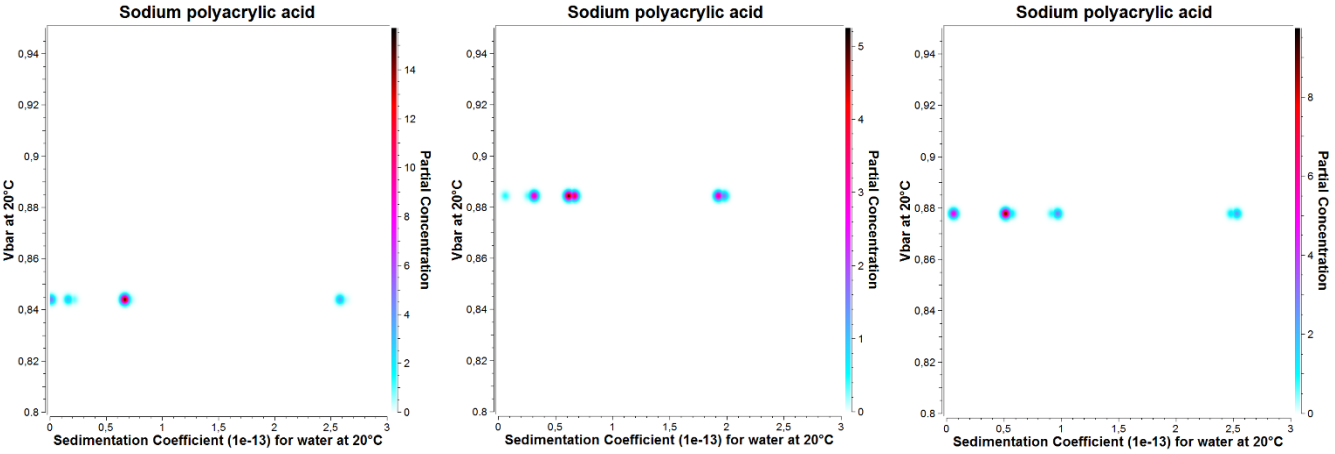

Figure S8: Pseudo-3D plots of the analysis of the AUC data of NaPAA using ULTRASCAN PCSA. Plotted is the sedimentation coefficient against $\bar{\nu}$, each model for the best fit which was obtained.

4. Analysis of the silver clusters

The graph of a repetition of the silver clusters synthesis, experiment and analysis is shown in Figure S9. Although not all the values are in agreement with the original plot in Figure 3, the range of the found species and the resolution is still the same and therefore support the found results.

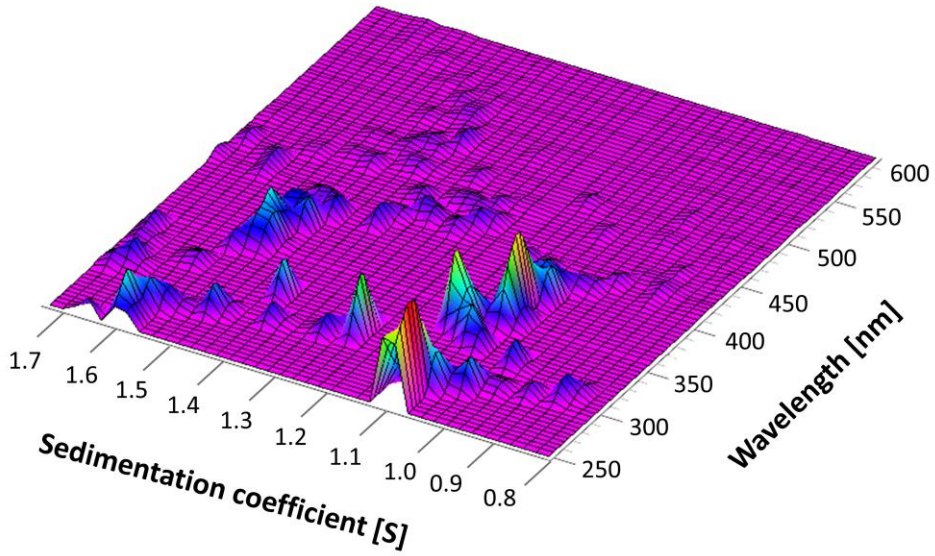

Figure S9: Analysis of a repetition of the silver cluster synthesis.

Individual spectra (normalized) for the different species from the multiwavelength (MWL) analysis of the silver clusters are graphed in Figure S10.

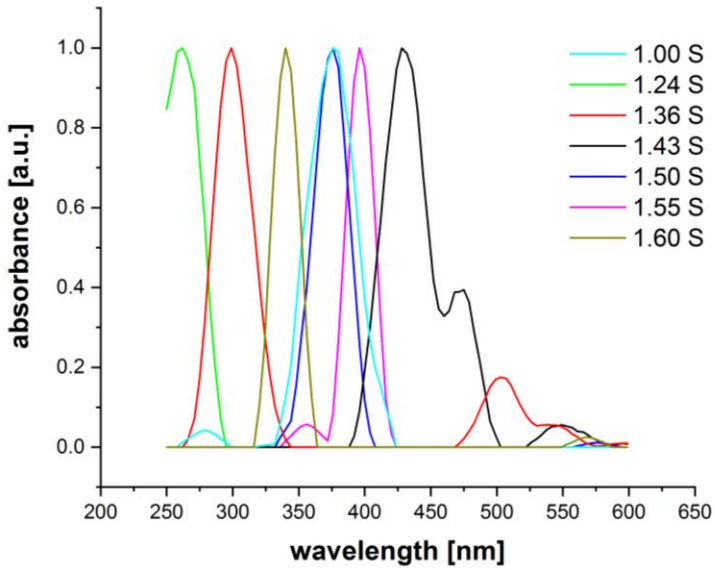

Figure S10: Normalized UV/vis spectra of the individual species from the MWL AUC analysis.

Some representative high-resolution transmission electron microscopy (HR-TEM) images of the silver clusters were recorded and are shown in Figure S11 and Figure S12.

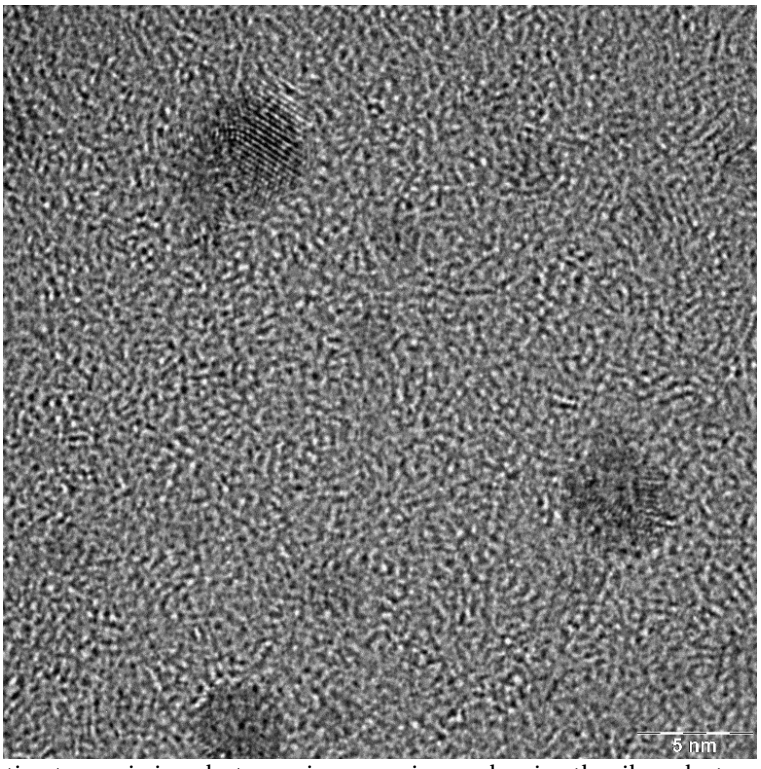

Figure S11: High-resolution transmission electron microscopy image showing the silver clusters. Visible are small particles, which are already at the resolution limit of the microscope.

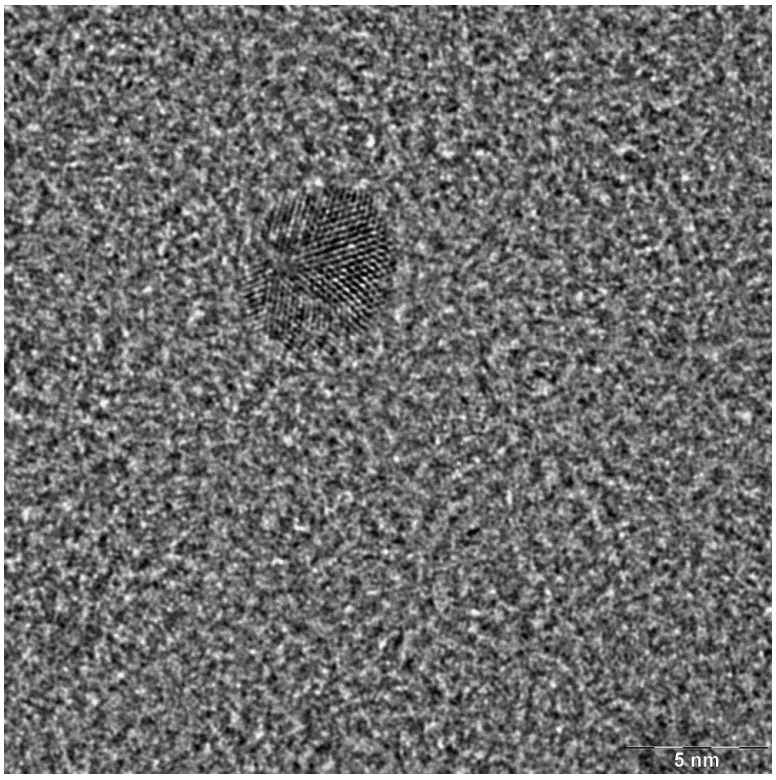

Figure S12: Another representative high-resolution transmission electron microscopy image of the silver clusters. The different lattice planes are visible, which seem to have different orientation within the particle, suggesting it is coalesced of different clusters.

Analysis in ULTRASCAN using PCSA-DS provided the following results for representative wavelengths, showing a plot of the sedimentation coefficient against $\bar{v}$, which were the values fitted for, for each individual wavelength (Figure S13). The values of the plots are listed in Table S1.

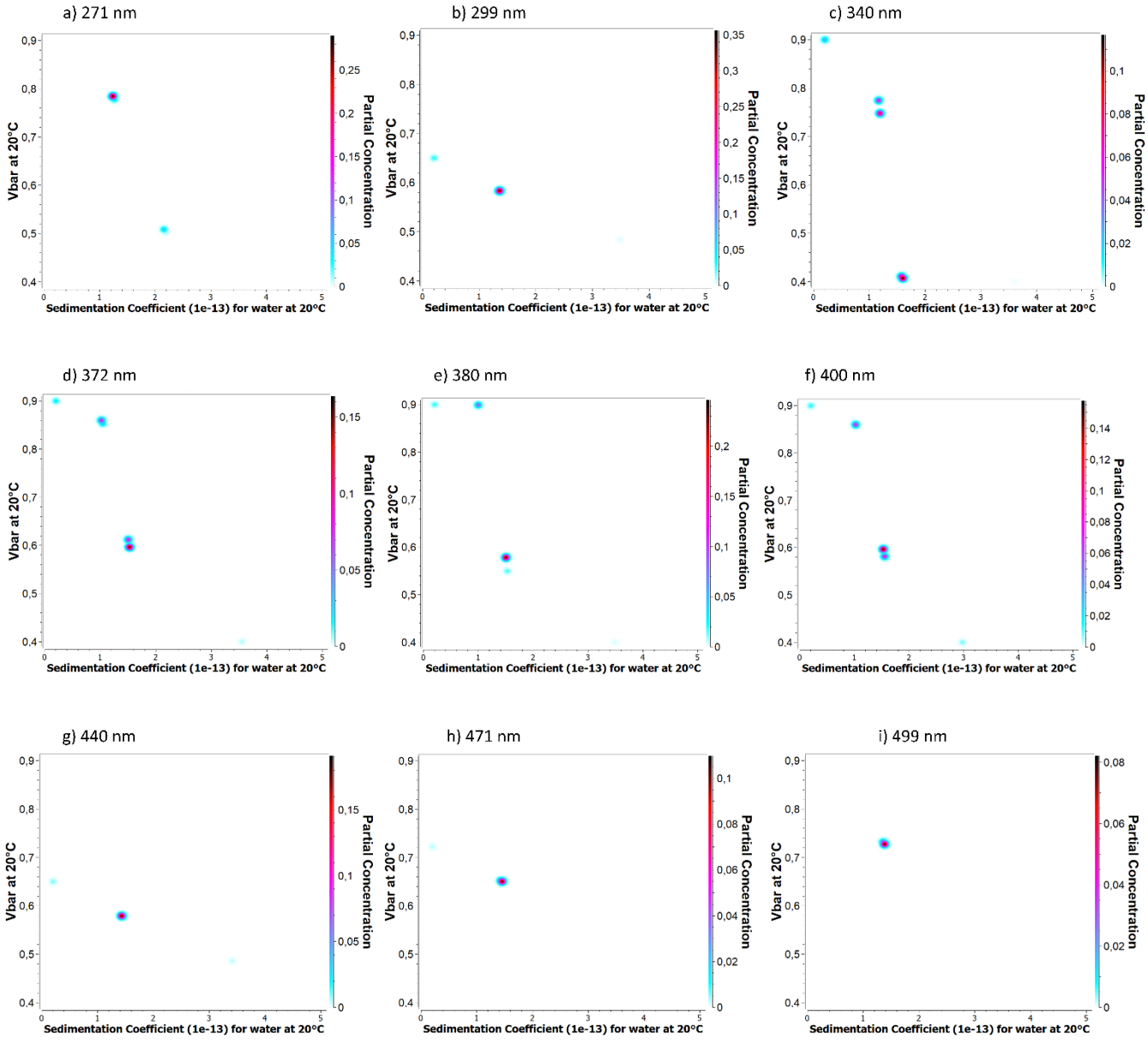

Figure S13: Analysis of silver clusters with ULTRASCAN. Shown are the fits for the sedimentation coefficient and $\bar{v}$ for representative wavelengths.

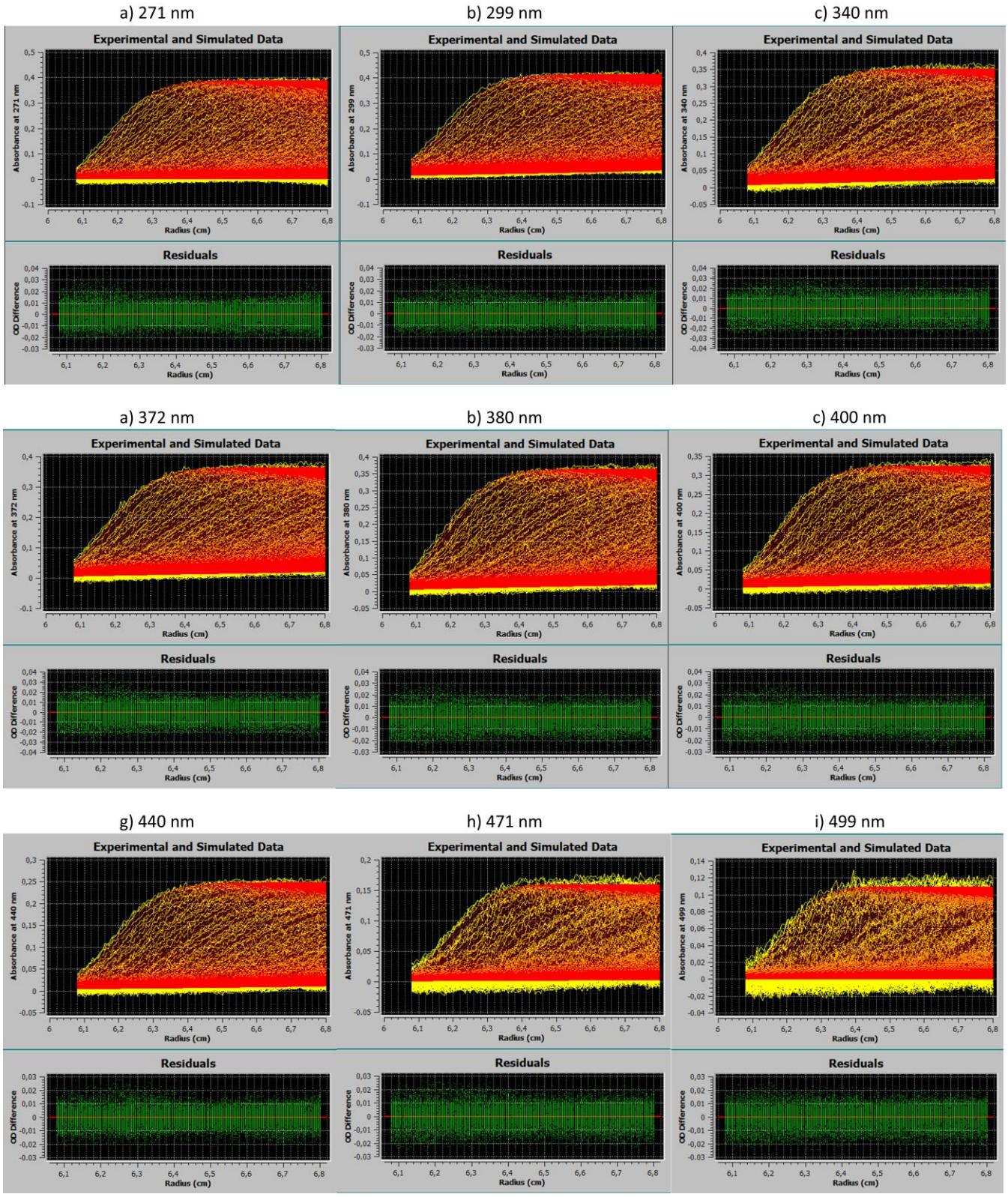

Figure S14: Ultrascan experimental and simulated data and the residuals for the PCSA-DS analysis of the silver clusters.

Table S1: Values of the ULTRASCAN analysis for each silver cluster for the fitted sedimentation coefficient and $\bar{\nu}$.

sedimentation coefficient [S]	wavelength λ_{max} [nm]	$\bar{\nu}$ [mL/g]	ρ [g/mL]
1.00	**370**	**0.86**	**1.16**
1.24	**270**	**0.78**	**1.28**
1.36	**300[1] + 500[2]**	**0.581/0.732**	**1.721/1.372**
1.43	**440[1] + 470[2]**	**0.581/0.652**	**1.721/1.542**
1.50	**380**	**0.58**	**1.72**
1.55	**400**	**0.58**	**1.72**
1.60	**340**	**0.41**	**2.44**

For the sedimentation coefficients 1.36 S and 1.43 S two values for $\bar{\nu}$ are obtained as these species are absorbing at two wavelengths (see second column). The first value ([1]), refers to the first wavelength, analogous for the second value.

The graph of the Monte-Carlo Fit of the PCSA-DS of the silver clusters is shown in Figure S15.

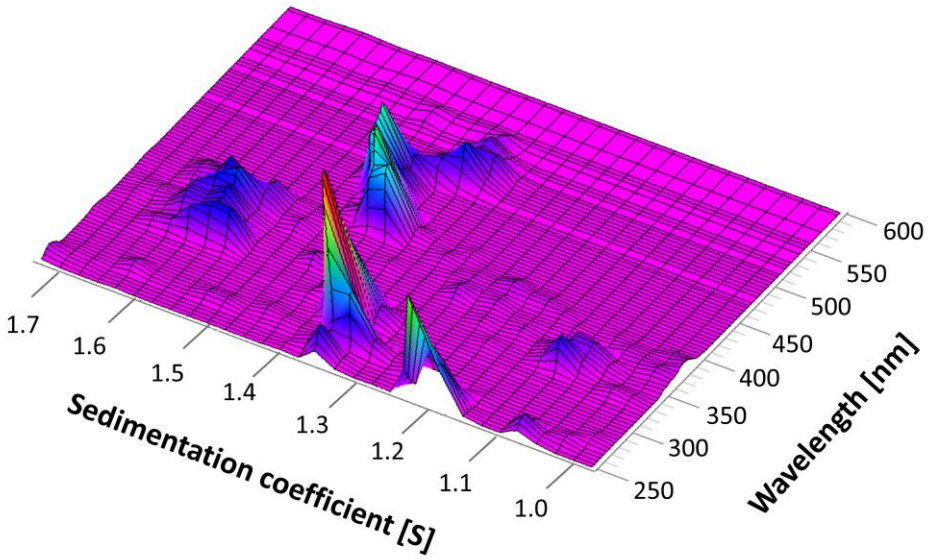

Figure S15: 3D plot of the PCSA-DS-MC analysis of the silver clusters.

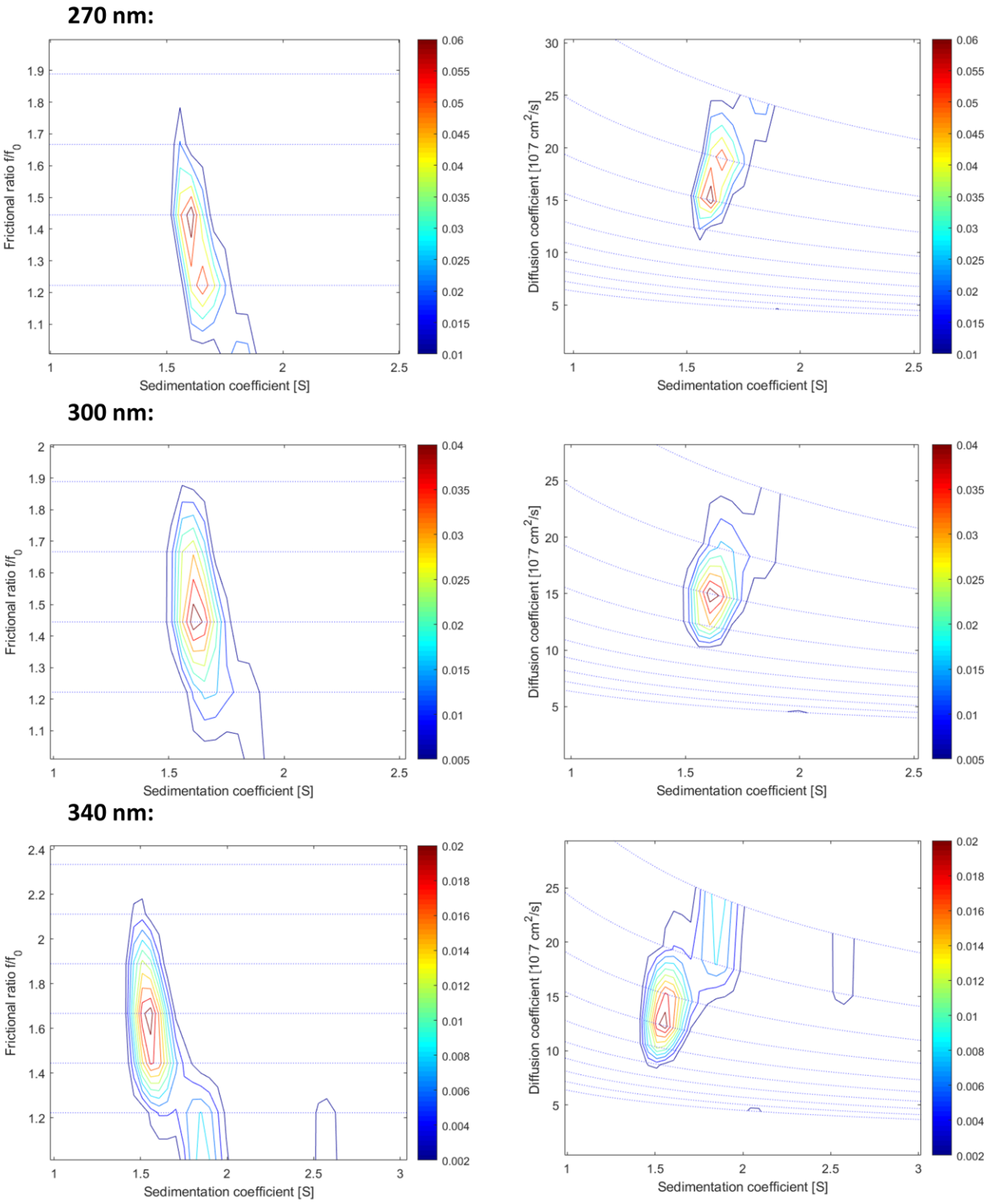

Figure S16: Results of the analysis of the silver clusters using the 2D analysis in SEDFIT for the relevant wavelengths 270 nm, 300 nm and 340 nm.

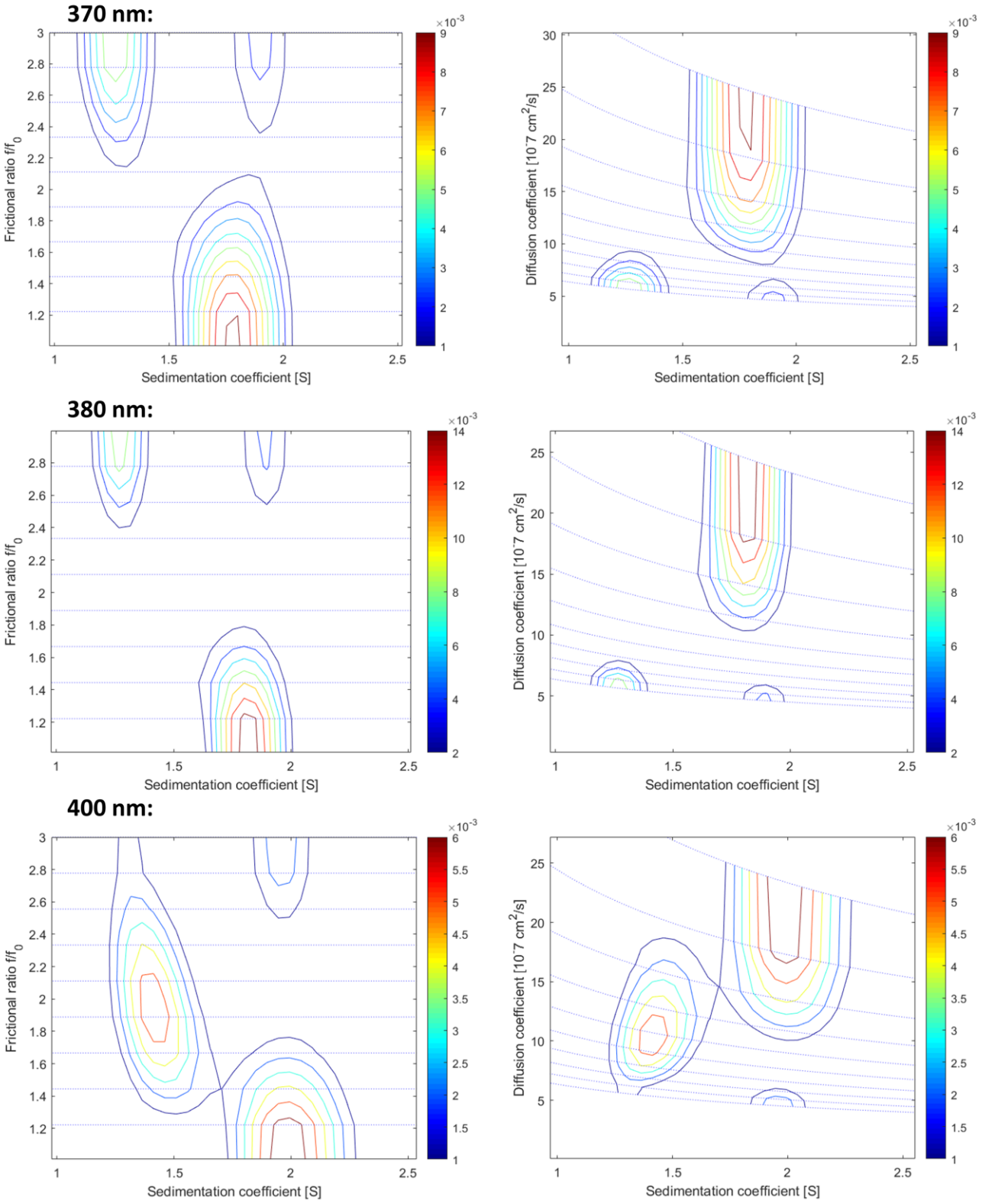

Figure S17: Results of the analysis of the silver clusters using the 2D analysis in SEDFIT for the relevant wavelengths 370 nm, 380 nm and 400 nm.

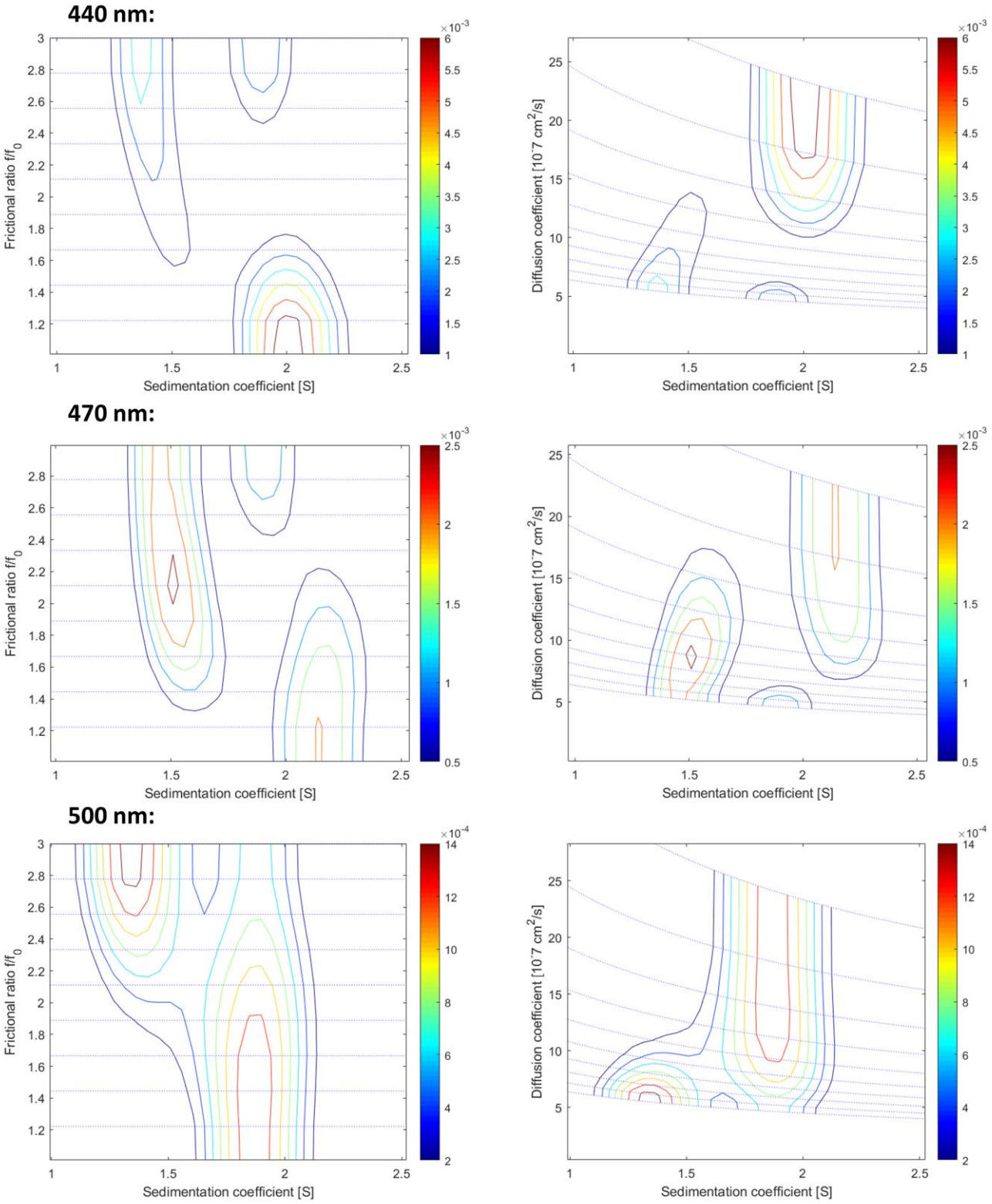

Figure S18: Results of the analysis of the silver clusters using the 2D analysis in SEDFIT for the relevant wavelengths 470 nm, 470 nm and 500 nm.

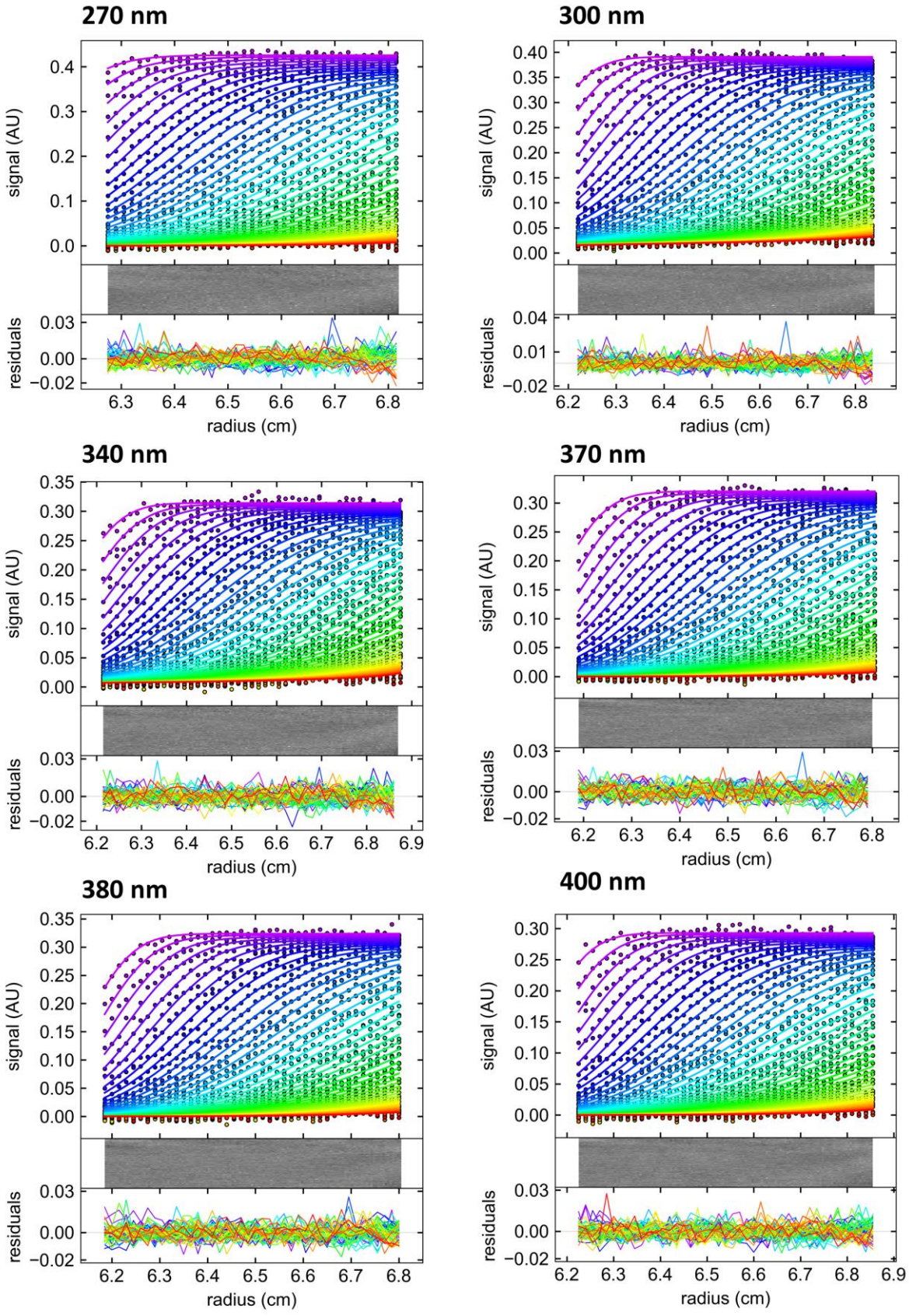

Figure S19: Data fits and residual plots of the analysis of the AUC data of the silver clusters using SEDFIT for the wavelengths 270, 300, 340, 370, 380 and 400 nm.

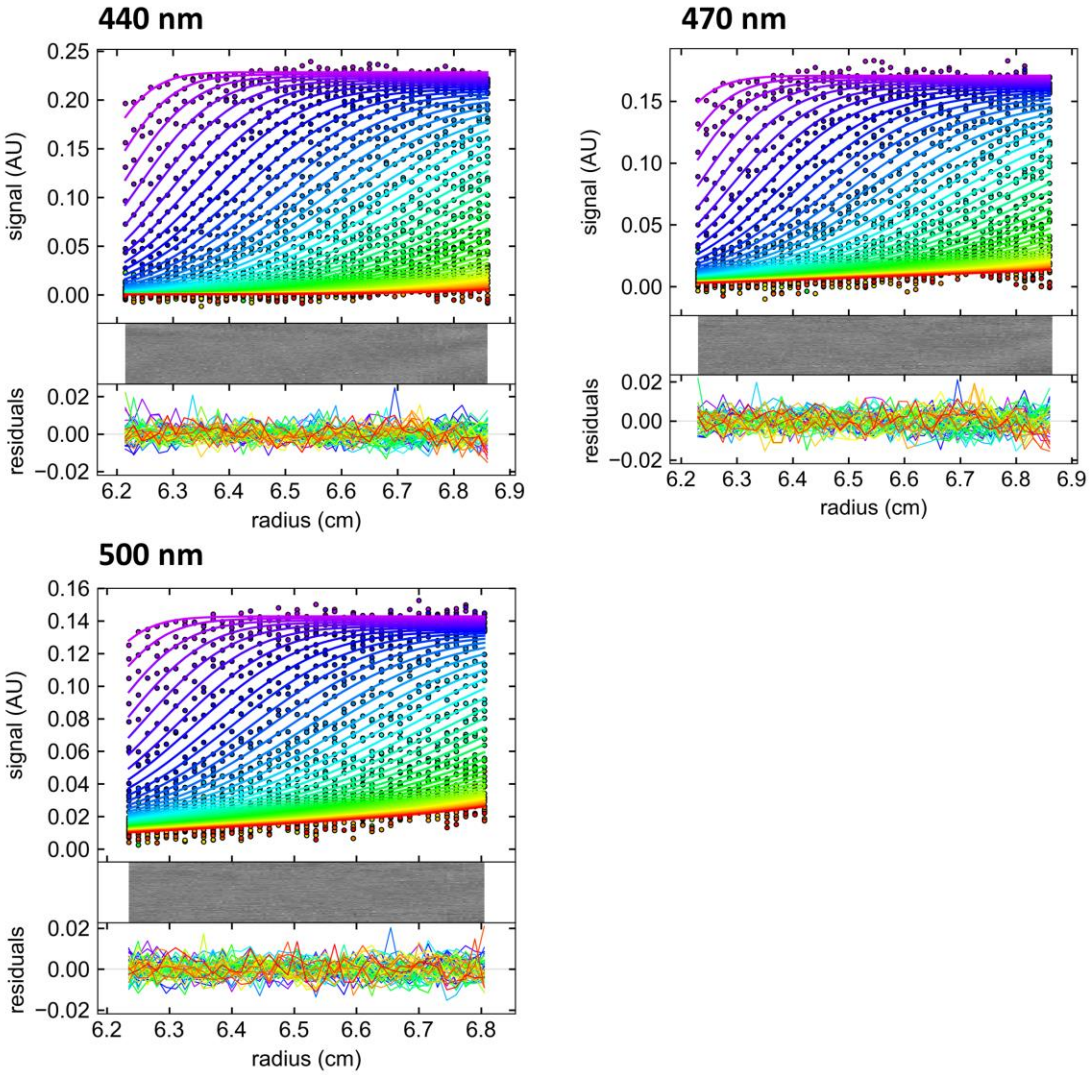

Figure S20: Data fits and residual plots of the analysis of the AUC data of the silver clusters using SEDFIT for the wavelengths 440, 470 and 500 nm.

In the following table, an overview of the SEDFIT analysis of the silver clusters is given.

Table S2: Values of the SEDFIT analysis for each silver cluster for the fitted sedimentation coefficient and $\bar{v}$.

sedimentation coefficient [S]	wavelength λ_{max} [nm]	$\bar{v}$ [mL/g]	f/f_o
1.51	470	0.92	2.1
1.55	340	0.85	1.7
1.60	500	0.88	2.9
1.63	300	0.81	1.45
1.66	270	0.74	1.45
1.75	380	0.72	1.1
1.78	370	0.68	1.1
1.81	400	0.74	1.1 + 1.9
2.01	440	0.65	1.1

In the following table, the values from the calculations using the core-shell models are shown.

Table S3: Results from the calculations based on the core-shell model. Column 2 and 3 show the calculations for core-shell model 1. NaPAA represents the shell with determined values, the core (Ag + H_2O) values are calculated based on the average overall particle density (1.57 g/mL). The calculations for core-shell model 2 are shown in column 4 + 5. Based on the known densities of the H_2O shell (0.99704 g/mL) and the bulk silver core (10.49 g/mL), the volume ratios were calculated. From those, the radius was determined.

s_{app} [S]	ρ core (Ag + H_2O) [g/mL]	r core (Ag + H_2O) [nm]	r core (Ag) [nm]	r shell (H_2O) [nm]
1.28	1.35	0.63	0.21	0.42
1.56	1.39	0.72	0.25	0.47
1.72	1.41	0.78	0.27	0.51
1.81	1.42	0.81	0.29	0.52
1.90	1.42	0.83	0.29	0.54
1.96	1.43	0.85	0.30	0.55
2.02	1.43	0.87	0.31	0.56

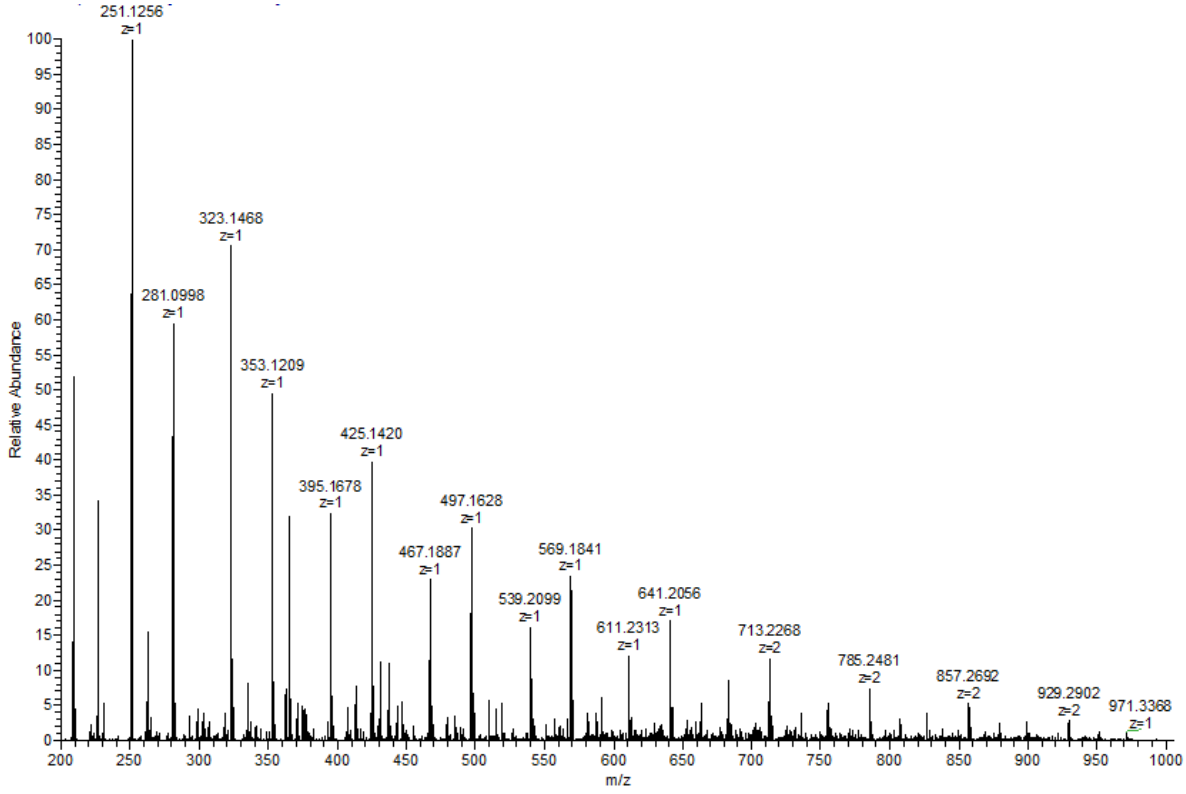

Figure S21: ESI-MS spectrum of the silver clusters. The mass of a single silver atom is 108 u.

5. Core-shell model for size evaluation

To calculate the size of the silver core, a core-shell model is applied. This relies on the assumption that the overall density of the particle consists proportionately of the shell density and core density, which in our case refers to the density of the silver core ρ_{core} (10.49 g/mL) and the NaPAA shell ρ_{shell} (1.15 g/mL). The ratio is determined by the respective volume fraction of the overall particle .This relates to the radius fraction to the power of three (in case of a spherical particle) and can be also described by the following formula:

$$\bar{v}_P = r^3\left(\rho_{core} \cdot {r_{core}}^3 + \rho_{shell}(r^3 - {r_{core}}^3)\right)^{-1}$$

$\bar{v}_P$ refers to the partial specific volume of the overall particle, r to the radius of the overall particle and r_{core} to the radius of the core. The volume fraction of each component can be used to calculate the overall density. From AUC analysis of the silver clusters the sedimentation coefficient s of each cluster is determined, which can be used to calculate the radius of the overall particle with previous knowledge of the density of the overall particle ($\rho_P = \bar{v}_P{}^{-1}$) by $2r = \sqrt{\frac{18\eta_S s}{\rho_P - \rho_S}}$. In our case, the overall density is not well determined, but the fraction the shell contributes to the overall radius (2.5 nm) and density (1.15 g/mL) is known as well as the core density. Using these values and the model described above, sedimentation coefficients can be calculated under variation of the core size. The sedimentation coefficient, which matches the value obtained from analysis gives back the respective core size which applies to the evaluated particle.

This way, the core radius can be calculated based on the sedimentation coefficient of the particle, knowledge of the solvent (ρ_s = 0.99704 g/mL and η_s = 0.00891 P), the density of the core and the density and thickness of the surfactant layer ($r_P - r_{core}$).

6. References

1. Henglein, A.; Linnert, T.; Mulvaney, P. Reduction of Ag+ in Aqueous Polyanion Solution: Some Properties and Reactions of Long-Lived Oligomeric Silver Clusters and Metallic Silver Particles. *Berichte der Bunsengesellschaft für physikalische Chemie* **1990,** *94* (12), 1449-1457.
2. Strauss, H.; Karabudak, E.; Bhattacharyya, S.; Kretzschmar, A.; Wohlleben, W.; Cölfen, H. Performance of a fast fiber based UV/vis multiwavelength detector for the analytical ultracentrifuge. *Colloid. Polym. Sci.* **2008,** *286* (2), 121-128.
3. Walter, J.; Löhr, K.; Karabudak, E.; Reis, W.; Mikhael, J.; Peukert, W.; Wohlleben, W.; Cölfen, H. Multidimensional Analysis of Nanoparticles with Highly Disperse Properties Using Multiwavelength Analytical Ultracentrifugation. *ACS Nano* **2014,** *8* (9), 8871-8886.
4. Bhattacharyya, S. K.; Maciejewska, P.; Börger, L.; Stadler, M.; Gülsün, A. M.; Cicek, H. B.; Cölfen, H. Development of fast fiber based UV-Vis multiwavelength detector for an ultracentrifuge. *Prog. Colloid Polym. Sci.* **2006,** *131*, 9-22.
5. Pearson, J.; Walter, J.; Peukert, W.; Cölfen, H. Advanced Multiwavelength Detection in Analytical Ultracentrifugation. *Anal. Chem.* **2018,** *90* (2), 1280-1291.
6. Demeler, B. UltraScan - A Comprehensive Data Analysis Software Package for Analytical Ultracentrifugation Experiments. In *Analytical Ultracentrifugation: Techniques and Methods*, Scott, D. J.; Harding, S. E.; Rowe, A. J., Eds. The Royal Society of Chemistry: 2005; pp 210-230.
7. Schuck, P. Size-Distribution Analysis of Macromolecules by Sedimentation Velocity Ultracentrifugation and Lamm Equation Modeling. *Biophys. J.* **2000,** *78* (3), 1606-1619.
8. Gorbet, G.; Devlin, T.; Hernandez Uribe, Blanca I.; Demeler, Aysha K.; Lindsey, Zachary L.; Ganji, S.; Breton, S.; Weise-Cross, L.; Lafer, Eileen M.; Brookes, Emre H.; Demeler, B. A Parametrically Constrained Optimization Method for Fitting Sedimentation Velocity Experiments. *Biophys. J.* **2014,** *106* (8), 1741-1750.
9. Carney, R. P.; Kim, J. Y.; Qian, H.; Jin, R.; Mehenni, H.; Stellacci, F.; Bakr, O. M. Determination of nanoparticle size distribution together with density or molecular weight by 2D analytical ultracentrifugation. *Nature Communications* **2011,** *2*, 335.
10. Karabudak, E.; Brookes, E.; Lesnyak, V.; Gaponik, N.; Eychmüller, A.; Walter, J.; Segets, D.; Peukert, W.; Wohlleben, W.; Demeler, B.; Cölfen, H. Simultaneous Identification of Spectral Properties and Sizes of Multiple Particles in Solution with Subnanometer Resolution. *Angew. Chem. Int. Ed.* **2016,** 55 (39), 11770-11774.